

# Calculations of Hubbard $U$ from first-principles.

F. Aryasetiawan<sup>1,2</sup>, K. Karlsson<sup>3,4</sup>, O. Jepsen<sup>4</sup> and U. Schonberger<sup>4</sup>,

<sup>1</sup>Research Institute for Computational Sciences, AIST,

Umezono 1-1-1, Tsukuba Central 2, Tsukuba Ibaraki 305-8568 Japan,

<sup>2</sup>CREST, Japan Science and Technology Agency

<sup>3</sup>Department of Natural Science,

Hogskolan i Skovde, 54128 Skovde, Sweden

<sup>4</sup>Max Planck Institut für Festkörperforschung and

D-705 06 Stuttgart, Germany

(Dated:)

## Abstract

The Hubbard  $U$  of the 3d transition metal series as well as  $\text{SrVO}_3$ ,  $\text{YTiO}_3$ , Ce and Gd has been estimated using a recently proposed scheme based on the random-phase approximation. The values obtained are generally in good accord with the values often used in model calculations but for some cases the estimated values are somewhat smaller than those used in the literature. We have also calculated the frequency-dependent  $U$  for some of the materials. The strong frequency dependence of  $U$  in some of the cases considered in this paper suggests that the static value of  $U$  may not be the most appropriate one to use in model calculations. We have also made comparison with the constrained LDA method and found some discrepancies in a number of cases. We emphasize that our scheme and the constrained LDA method theoretically ought to give similar results and the discrepancies may be attributed to technical difficulties in performing calculations based on currently implemented constrained LDA schemes.

## I. INTRODUCTION

Many-electron problem in real materials is too complicated to be tackled directly from first principles. Direct conventional methods for calculating excited-state properties are available and one of the most successful among these is the GW approximation (GWA) [1, 2]. However, it has proven difficult to go beyond the GWA purely from first principles for a number of reasons. Seen from diagrammatic point of view, the GWA is a sum of bubble diagrams corresponding to the random-phase approximation (RPA) [3], which can be more generally regarded as time-dependent Hartree approximation. Firstly it is far from obvious which classes of diagrams should be included beyond the RPA. Secondly when we do include another class of diagrams, the lowest order diagram, i.e., second order, is likely to be included twice. This is because there are only very few lower order diagrams so that different classes of diagrams will tend to have an overlap of the lowest-order diagrams. This double counting has to be taken into account. However, for an arbitrary frequency, the imaginary part of the second-order self-energy may be larger than, e.g., the imaginary part of the GW self-energy. When the second-order self-energy is subtracted for double counting this may lead to a wrong sign of the imaginary part of the self-energy with unphysical consequences such as a negative spectral function.

It is therefore worthwhile to consider an alternative approach of tackling the many-electron problem in real materials. We note that of the large number of degrees of freedom only a few are actually relevant for electron correlations. A typical problem that is difficult to treat with conventional methods corresponds to a system with localized orbitals embedded in extended states. Many so-called strongly correlated materials, such as perovskites, are of this type, consisting of localized 3d or 4f orbitals embedded in extended s-p states. Electrons living in the localized orbitals experience strong correlations among each other with a subtle coupling to the extended states resulting in a complicated many-electron problem. The RPA is probably insufficient for treating correlations among electrons in localized orbitals. One may speculate that many classes of diagrams contribute with similar weight to correlations, making it very difficult to go beyond the RPA by including a few extra classes of diagrams.

The idea of isolating a few degrees of freedom relevant for correlation has been utilized for many years in the Hubbard model or the Anderson impurity model. Renormalized or screened Coulomb interaction (Hubbard  $U$ ) is kept among electrons living in the localized

orbitals. In the Anderson model some states coupled to the localized orbitals are also kept but without Coulomb interaction and the rest of the states are downfolded resulting in a renormalized Coulomb interaction. Although the physical picture seems clear it is not immediately evident how to calculate the Hubbard  $U$ . Indeed in practice it has usually been regarded as an adjustable parameter. Adjustable parameters are unsatisfactory since they limit the quantitative predictive power of the model. Even qualitatively adjustable parameters might lead to misleading conclusions. It is therefore highly desirable to find a systematic way of calculating the parameters in the Hubbard model, in particular the Hubbard  $U$ , from realistic electronic structure calculations.

The problem of determining the Hubbard  $U$  from first principles has been addressed by a number of authors. One of the earliest works is the constrained local density approximation (cLDA) approach [4, 5, 6] where the Hubbard  $U$  is calculated from the total energy variation with respect to the occupation number of the localized orbitals. A further improvement of this scheme was recently proposed [7, 8, 9]. A different approach based on the random-phase approximation (RPA) was later introduced [10], which allows for the calculations of the matrix elements of the Hubbard  $U$  and its energy dependence. More recently, it was shown that it is possible to calculate the Hubbard  $U$  systematically from first principles [11]. It was soon realized that these two methods of calculating the Hubbard  $U$ , RPA and cLDA, do not yield the same results. This is very puzzling since the two approaches are supposed to give the effective interaction of the localized electrons and ought to give the same results.

The purpose of the present work is to present results for the Hubbard  $U$  of the 3d series and a few other materials (Ce,  $\text{SrVO}_3$ ,  $\text{YTiO}_3$ ) and to analyze the origin of the discrepancy between RPA and cLDA results.

## II. THEORY

### A. Constrained RPA

The fully screened Coulomb interaction is given by

$$W = [1 - vP]^{-1} v \quad (1)$$

where  $v$  is the bare Coulomb interaction and  $P$  is the non-interacting polarization given by

$$P(\mathbf{r}; \mathbf{r}^0; \omega) = \sum_{i,j} \psi_i(\mathbf{r}) \psi_i(\mathbf{r}^0) \psi_j(\mathbf{r}) \psi_j(\mathbf{r}^0) \frac{1}{\omega - \epsilon_j + \epsilon_i + i0^+} - \frac{1}{\omega - \epsilon_j - \epsilon_i - i0^+} : \quad (2)$$

where  $\psi_i, \epsilon_i$  are one-particle Bloch eigenfunctions and eigenvalues corresponding to the system's band structure. For systems with a narrow 3d or 4f band across the Fermi level, typical of strongly correlated materials, we may divide the polarization into  $P = P_d + P_r$ , in which  $P_d$  includes only 3d to 3d transitions (i.e., limiting the summations in (2) to  $i, j \in f_{3d}$ ), and  $P_r$  be the rest of the polarization. In a previous publication [11] it was shown that the following quantity can be interpreted as the effective interaction among electrons living in the narrow band (Hubbard  $U$ ):

$$U(\omega) = [1 - v P_r(\omega)]^{-1} v \quad (3)$$

where  $U$  can be related to the fully screened interaction  $W$  by the following identity:

$$W = [1 - U P_d]^{-1} U : \quad (4)$$

This identity explicitly shows that the interaction between the 3d electrons is given by a frequency-dependent interaction  $U$ . Thus the remaining screening channels in the Hubbard model associated with the 3d electrons, represented by the 3d-3d polarization  $P_d$ ; further screen  $U$  to give the fully screened interaction  $W$ . In analogy to the constrained LDA method, we refer the method of calculating the Hubbard  $U$  as in (3) as "constrained RPA" (cRPA) because we have constrained the polarization to exclude 3d-3d transitions. In contrast to Ref. [8], it is not necessary to subtract the contribution arising from rehybridization of the non-interacting Kohn-Sham band structure because the wave functions and eigenvalues appearing in Eq. (2) are fixed.

It is noteworthy that  $U$  in Eq. (3) is a function of positions  $\mathbf{r}$  and  $\mathbf{r}'$ , independent of basis functions. This is because the polarization in Eq. (2) depends on the Bloch wave functions and eigenvalues, which can be calculated in any basis. Thus, our method is basis-independent. In the following, we retain only the local components of the effective interaction on the same atomic site by taking the following matrix element:

$$U = \int d^3 r d^3 r^0 \int_{3d} \psi_{3d}(\mathbf{r}) \int U(\mathbf{r}; \mathbf{r}^0) \int_{3d} \psi_{3d}(\mathbf{r}^0) \int \quad (5)$$

where  $\phi_{3d}$  is a 3d LMTO [12] orbital centered on an atomic site and the interaction  $U(\mathbf{r}; \mathbf{r}^0)$  is the static ( $\omega = 0$ ) value of Eq. (3). In calculating  $U$  we have approximated  $\phi_{3d}$  by the "head" of the LMTO, i.e., the solution to the Schrodinger equation inside the atomic sphere. This is expected to be a reasonable approximation because the 3d states are rather localized. The lattice Hubbard model with a static interaction  $U$  is given by

$$H = \sum_{\mathbf{R}n, \mathbf{R}'n'} c_{\mathbf{R}n}^\dagger h_{\mathbf{R}n, \mathbf{R}'n'} c_{\mathbf{R}'n'} + \frac{1}{2} \sum_{\mathbf{R}n, \mathbf{R}'n'} c_{\mathbf{R}n}^\dagger c_{\mathbf{R}'n'} U_{nn'} c_{\mathbf{R}n'}^\dagger c_{\mathbf{R}'n'} \quad (6)$$

$h_{\mathbf{R}n, \mathbf{R}'n'}$  is the one particle part of the Hamiltonian consisting of hopping and the orbital energy. A model with a frequency-dependent  $U$  can be formulated within the action integral approach but cannot be formulated within the Hamiltonian approach [11]. It is clear that the  $U$  entering the Hubbard model will inevitably depend on the choice of the one-particle basis  $\phi_{3d}$  defining the annihilation and creation operators, no matter what method we use to calculate  $U(\mathbf{r}; \mathbf{r}^0)$ . LMTO is just one possible choice for the one-particle orbitals but other choices are perfectly legitimate. For example, the newly developed NMTO ( $N$  corresponds to the order of the Taylor expansion in energy of the orbital) [13] and the recently proposed maximally localized Wannier orbitals [14] are possible choices.

## B. Constrained LDA

The derivative of the total energy with respect to an occupation number  $n_i$  of a given state can be related to its Kohn-Sham eigenvalue as follows [15]:

$$\frac{\partial E}{\partial n_i} = \epsilon_i \quad (7)$$

From the Kohn-Sham equation [16] one can show that following relation holds [10, 17]

$$\frac{\partial \epsilon_i}{\partial n_j} = \frac{\partial^2 E}{\partial n_i \partial n_j} = \delta_{ij} (v + f_{xc})^{-1} \delta_{ij} \quad (8)$$

where

$$f_{xc}(\mathbf{r}; \mathbf{r}^0) = \frac{\partial^2 E_{xc}}{\partial \rho(\mathbf{r}) \partial \rho(\mathbf{r}^0)} = \frac{\partial v_{xc}(\mathbf{r})}{\partial \rho(\mathbf{r}^0)}$$

and  $\epsilon^{-1}$  is the inverse dielectric function which can be expressed in terms of the linear density-density response function  $R = \delta n_{\text{ext}} / \delta v_{\text{ext}}$ ; i.e., the change in density with respect to an external perturbation  $v_{\text{ext}}$ , as

$$\epsilon^{-1} = 1 + Rv.$$

The integral in (8) is defined as

$$W_{ij} = \int d^3r d^3r^0 \psi_i(r) \psi_j(r^0) F(r; r^0) \psi_j(r^0) \psi_i(r). \quad (9)$$

Within the RPA, which is equivalent to time-dependent Hartree approximation,  $f_{xc} = 0$  implying that  $(v + f_{xc})^{-1} = v + vRv = W$ ; i.e., the change in the Kohn-Sham eigenvalue is directly related to the screened interaction. In fact in practice  $f_{xc} \ll v$  so that to a good approximation we may assume that  $\epsilon_{ij}^{-1} = W_{ij}$ :

The idea in a constrained LDA calculation (cLDA) is to perform a self-consistent (super-cell) total energy calculation with a constrained 3d occupancy on the so called impurity atom. Furthermore, the coupling between the impurity (3d-level) and the rest of the system, which is explicitly included in the model Hamiltonian, is removed in order to avoid double counting. According to (8) the Hubbard  $U$  is then given by the change in the 3d-level when the number of localized 3d electrons are varied and the hopping for the localized 3d electrons is suppressed:

$$U = \frac{\partial C_{3d}}{\partial n_{3d}}; \quad (10)$$

where  $C_{3d}$  is the center of the 3d band. By suppressing the hopping of the 3d electrons, the screened interaction so obtained corresponds to an effective interaction without the participation of screening from the 3d electrons, which is what we mean by the Hubbard  $U$ . However, by cutting off the hopping of the 3d electrons, we do not only eliminate hopping to 3d bands but also hopping to bands other than 3d. We will elucidate later that the neglect of the latter hopping is the main origin of the discrepancy between cLDA and cRPA.

Within the LMTO-ASA (Atomic Sphere Approximation) scheme, the 3d level, or in fact the band-center  $C_{3d}$ , is obtained by solving the radial Schrodinger equation for the impurity atom using  $\infty$  boundary condition (BC) at the muffin-tin (MT) sphere [12]. The

BC are arbitrarily chosen so the radial wavefunction in the sphere  $r_{3d}$  matches smoothly to  $r^{-1/2}$  at the MT sphere, which corresponds to a logarithmic derivative for the 3d-states of  $D_1 = 1 - 1 = -3$ . We note that in the above definition  $\epsilon_{3d}$  is allowed to relax (self-consistently) upon a change in the 3d charge. A decrease in the number of 3d electrons will make the potential more attractive and consequently the wavefunction will contract. This effect is compensated due to remaining electrons located outside the impurity sphere, which tend to screen. In addition we have performed so called modified U calculations using a fixed wavefunction, obtained in an ordinary bulk calculation, in order to make sure that the wavefunction  $\psi_{3d}$  coincides with the one used in the cRPA approach. Then the definition of U has to be slightly modified (denoted cLDA (modified) in Fig. (9)), and defined as the change in the expectation value of the impurity potential related to changes in 3d occupancy:

$$U = \frac{\partial \langle \psi_{3d} | V | \psi_{3d} \rangle}{\partial n_{3d}} = \frac{\partial}{\partial n_{3d}} \int d^3r \psi_{3d}^2(r) V(r) : \quad (11)$$

The above formula is obtained by observing that to first order in the perturbing potential the change in  $\epsilon_{3d}$  or  $C_{3d}$  is given by  $\langle \psi_{3d} | V | \psi_{3d} \rangle$ . In order to validate such a procedure for evaluating U, we have also adopted a scheme where firstly the supercell calculation is done until self-consistency using the fixed bulk wave functions, i.e., we perform a constrained calculation as usual but with fixed wave functions. Secondly the resulting self-consistent potential is used only once (BC  $D_1 = -3$ ) to obtain the  $C_{3d}$  level by solving the radial Schrodinger equation. Our results confirm that the value of U obtained from Eq. (10) using this one-shot iteration for the  $C_{3d}$  level is in fact the same as the value obtained from the modified definition in Eq. (11).

We must have in mind that in the LMTO-ASA method [12], any polarization of the screening charge is neglected. However, the screening charge inside the atomic sphere (on-site screening) is taken care of with good accuracy, but the non-local screening from other spheres is merely due to point-charges located at the sphere-centers (Madelung screening). In reality, this charge is expected to be located somewhat closer to the impurity sphere, thus reducing the value of the calculated U. As a consequence systems with almost all screening charge inside the impurity sphere are expected to be well described.

The beauty of the LMTO method is that the basis used in the band structure calculation is the same as the one-particle basis defining the annihilation and creation operator of the Hubbard model. Thus by constraining the occupation number of the orbital one directly

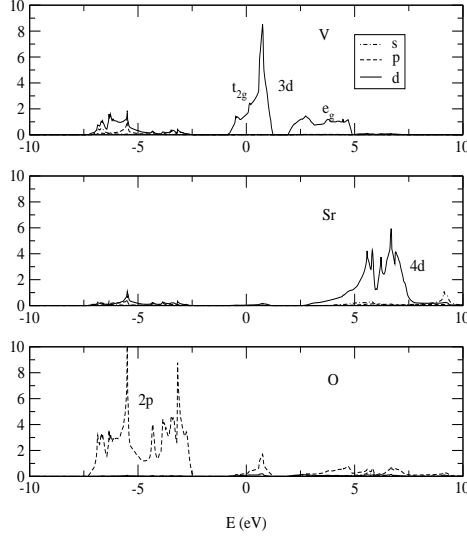


FIG. 1: Partial density of states of  $\text{SrVO}_3$ :

obtains the corresponding  $U$  from the change in the orbital energy with respect to the occupation number as in Eq. (8) or (10). This is in contrast to methods not based on localized orbitals, [8, 9] where projection to some localized orbitals defining the one-particle basis of the model Hamiltonian is necessary.

### III. RESULTS AND DISCUSSIONS

#### A. $\text{SrVO}_3$

$\text{SrVO}_3$  is an ideal case because across the Fermi level there is a narrow band of mainly  $t_{2g}$  character originating from V 3d, well separated from other bands. This allows for an unambiguous application of Eq. (3). To aid in visualizing the various transitions between occupied and unoccupied states the partial density of states of  $\text{SrVO}_3$  are displayed in Fig. 1. The effects of various possible screening channels on the value of the screened interaction are calculated systematically and shown in Fig. 2. From the figure we can read the value of  $U$  for the  $t_{2g}$  band, namely,  $U = 3.5$  eV. As can be seen from the figure, eliminating transitions from  $t_{2g}$  band to  $e_g$  band has hardly any effect on  $U$ . This implies that the Hubbard  $U$  for a model with only  $t_{2g}$  orbitals (case 1) is approximately the same as the one for a model with both  $t_{2g}$  and  $e_g$  orbitals (case 2). In fact, eliminating all transitions from the  $t_{2g}$  band (case



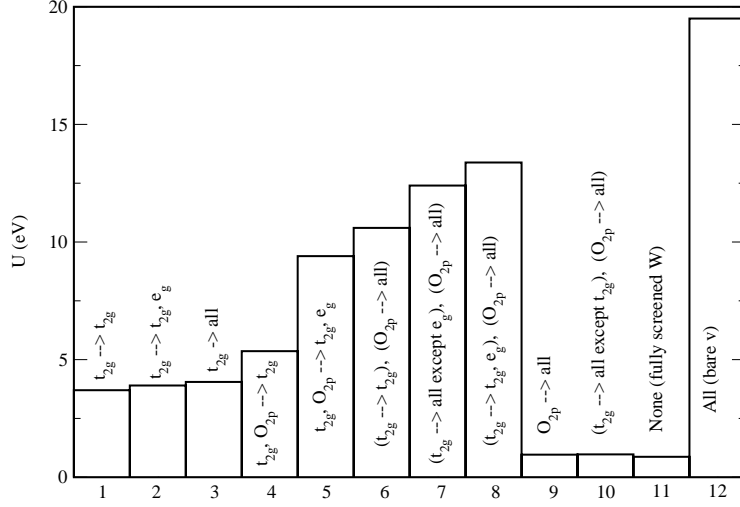


FIG. 2: The Hubbard  $U$  of  $\text{SrVO}_3$  obtained by eliminating various transitions as indicated in the picture. For example, case 5 corresponds to eliminating transitions  $t_{2g} \rightarrow t_{2g}$ ,  $t_{2g} \rightarrow e_g$ ,  $O_{2p} \rightarrow t_{2g}$ , and  $O_{2p} \rightarrow e_g$  and case 6 corresponds to eliminating  $t_{2g} \rightarrow t_{2g}$  transition and all transitions from  $O_{2p}$ . Discussion of the result is described in the text.

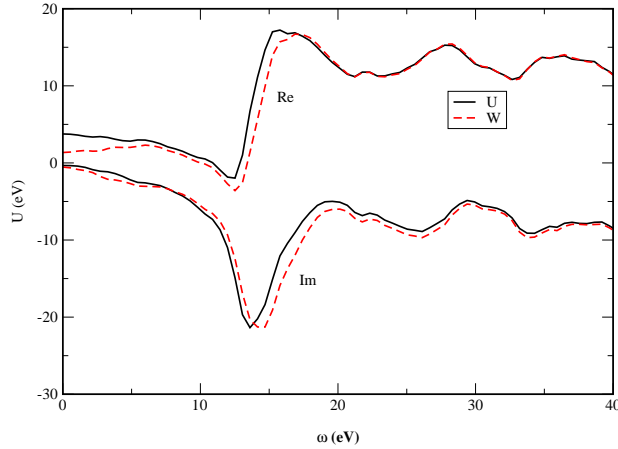


FIG. 3: Frequency dependent  $U$  and  $W$  of  $\text{SrVO}_3$ :

3) has little effect on  $U$ . This is because the small number of 3d electrons (1) contribute little to the polarization other than 3d-3d polarization. From cases 4, 5, and 6 it becomes evident that screening from the oxygen 2p electrons is very important. In particular, the transitions from oxygen 2p to  $t_{2g}$  and  $e_g$  bands are most significant (see also a recent work of Solovyev and Imada [7]). However, cases 9 and 10 are surprising: when all transitions

from the oxygen 2p are eliminated, the resulting screened interaction is almost the same as the fully screened interaction  $W$  (case 11). This means that the  $t_{2g}$  electrons alone are very efficient in performing the screening so that after the  $t_{2g}$  electrons have performed the screening there is little left for the oxygen 2p electrons to screen. In retrospect, it is a reasonable result because  $t_{2g} \rightarrow t_{2g}$  screening is metallic, which is very efficient. Similarly, when the oxygen 2p electrons are allowed to screen first (case 3), there is little left for the  $t_{2g}$  electrons to screen. Thus, cases 3 and 9 are not contradictory.

It is interesting to compare the value of  $U$  calculated using cRPA and cLDA. The value of  $U$  for the  $t_{2g}$  and  $e_g$  bands obtained from cLDA is 9.5 eV and the modified cLDA yields a value of 8.8 eV. Since in the implementation of cLDA, hopping to the 3d orbitals on a given impurity site in a supercell is prohibited, a fair comparison with cRPA would be to eliminate transitions from and to the 3d orbitals (both  $t_{2g}$  and  $e_g$ ). In this interpretation of cLDA, we should therefore make comparison with case 5, corresponding to the case where transitions from  $O_{2p}$  to 3d bands (both  $t_{2g}$  and  $e_g$ ) are also prohibited. Indeed the value corresponding to case 5 is very close to the modified cLDA value. We should also eliminate the  $t_{2g} \rightarrow \text{non-}t_{2g}$  screening but as shown by cases 1, 2, and 3 in Fig. (2), this screening channel is not important.

The frequency-dependent  $U$  and  $W$  are displayed in Fig. (3). There is a qualitative difference in the frequency dependence of the imaginary part of  $U$  of  $SrVO_3$  and late transition metals. In the former the imaginary part is dominated by a single plasmon excitation while the latter is characterized by a broad excitation with no distinct plasmon excitation. This is a consequence of the small polarization contribution of the  $t_{2g}$  electrons to non-3d orbitals in the former so that the plasmon excitation is dominated by the free-electron-like  $O_{2p}$ : In late transition metals, such as nickel, the 3d electrons themselves contribute very significantly to screening in the form of polarization to non-3d orbitals. The localized non-free-electron-like nature of the 3d electrons may be responsible for the broad excitation energies observed in  $\text{Im } U$  and  $\text{Im } W$ .

We have also calculated  $U$  for  $YTiO_3$  with a result equal to 4.0 eV. This value is significantly smaller than the value of 5.0 eV used in LDA+DMFT (Dynamical Mean-Field Theory) calculations. [18] The value of 5.0 eV is needed in order to open up a gap when starting from a metallic state in the LDA. While a smaller value of 3-4 eV would still be acceptable in the case of  $SrVO_3$  or  $CaVO_3$  since they are both metals, such value of  $U$  would

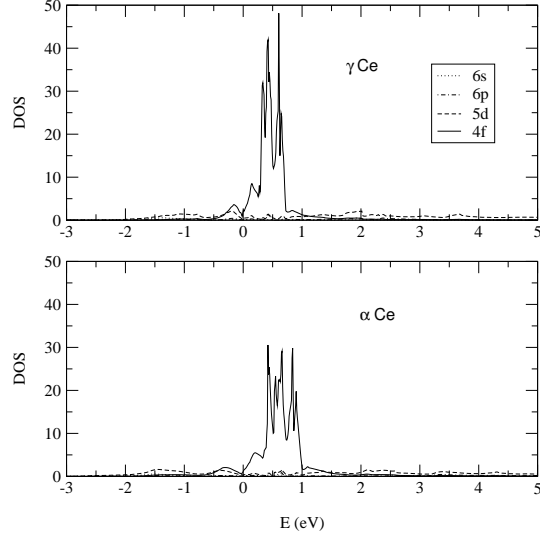


FIG. 4: Partial density of states of  $\gamma$ -Ce and  $\alpha$ -Ce.

just barely open up a gap in the case of  $\text{YTiO}_3$ . This poses a fundamental question concerning the value of the Hubbard  $U$  that is appropriate for DMFT. It could well be that due to the mapping to an impurity model, DMFT requires a larger  $U$  than the corresponding value for a lattice model. However, this runs counter to our intuition because by mapping to an impurity model one would expect that part of the screening process arising from the impurity's neighboring sites should already be included in the impurity  $U$ , which should therefore be smaller than the lattice  $U$ . Another possibility is that the RPA is not sufficient for treating local screening and more accurate approximation beyond the RPA may be needed. This question is now under study. We have also performed cLDA calculations giving a value of  $U = 7.5$  eV and 6.3 eV with a modified cLDA. We have not analyzed in detail the various transitions in  $\text{YTiO}_3$  since we believe they are essentially similar to those of  $\text{SrVO}_3$ .

#### B. Cerium

Another interesting case to consider is cerium although it is less ideal than  $\text{SrVO}_3$  due to a mixing between the 4f and 5d orbitals in the valence states. The partial densities of states of  $\gamma$ -Ce and  $\alpha$ -Ce are shown in Fig. 4. In Tables I and II the values of  $U$  for a number of energy windows are shown.

Energy window (eV)	U (eV)
(-2.0, 1.5)	7.9
(-1.5, 1.5)	7.6
(-1.0, 1.5)	5.7
(-0.5, 1.5)	3.3
(-0.5, 1.0)	2.9
(-0.5, 1.7)	3.3
(-0.5, 2.0)	3.4

TABLE I: U of Ce as a function of energy window

Energy window (eV)	U (eV)
(-2.0, 1.7)	6.6
(-1.5, 1.7)	5.4
(-1.0, 1.7)	4.3
(-0.7, 1.7)	3.2
(-0.7, 2.0)	3.3
(-0.7, 3.0)	3.4

TABLE II: U of Ce as a function of energy window

A reasonable choice of energy window for Ce and Ce are (-0.7, 1.7) and (-0.5, 1.5), respectively since these cover the 4f states. This choice gives a value of about 3.2–3.3 eV. It is clear from the tables that the value of U is very sensitive to the choice of the lower energy bound. Thus U is more than doubled when the lower bound is taken to be -2.0 eV, which corresponds to covering the entire occupied valence states. On the other hand, due to the small number of 4f electrons, U is not sensitive to the upper energy bound. This result is in reasonable accord with cLDA result of about 6 eV, which in our language corresponds to eliminating all transitions to and from the 4f states. Due to a slightly more extended 4f orbital, the result for Ce is somewhat smaller than that of Ce but otherwise they are very similar.

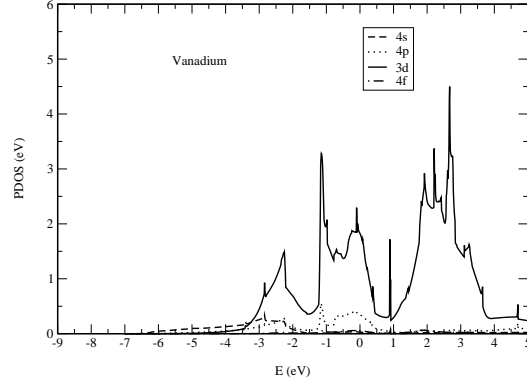


FIG . 5: Partial density of states of vanadium .

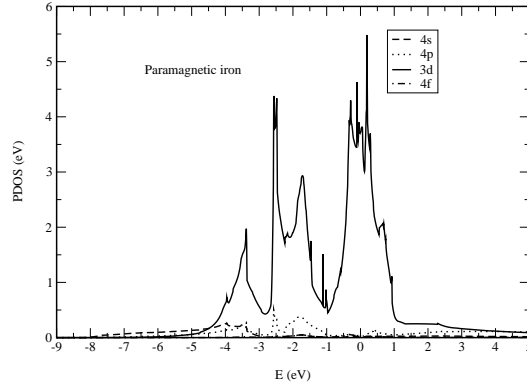


FIG . 6: Partial density of states of param agnetic iron .

### C . 3d transition m etal series

The Hubbard  $U$  for the 3d m etals is di cult to determ ine unam biguously because of the strong hybridization between the 3d and 4s-4p orbitals. Thus the result can depend strongly

Energy w indow (eV )	$U$ (eV )
(-2.0, 4.0)	3.7
(-3.0, 4.0)	6.3
(-4.0, 4.0)	7.0
(-2.0, 5.0)	3.8
(-2.0, 6.0)	3.9

TABLE III:  $U$  of V as a function of energy w indow

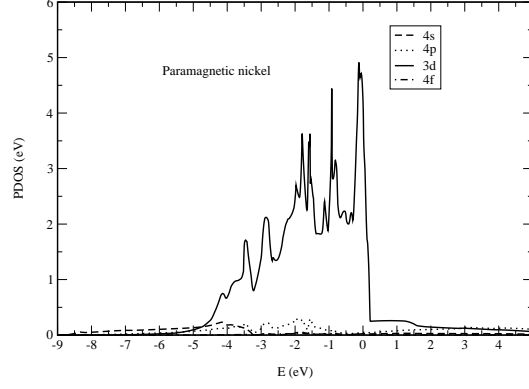


FIG . 7: Partial density of states of paramagnetic nickel.

Energy window (eV)	$U$ (eV)
(-3.0, 1.2)	4.0
(-4.0, 1.2)	4.8
(-5.0, 1.2)	5.0
(-3.0, 2.0)	4.3
(-3.0, 3.0)	5.3

TABLE IV :  $U$  of Fe as a function of energy window

on the energy window or on what we choose as our one-particle band in the Hubbard model. This is especially true in the early transition metals, as can be seen, for example, in Table III for vanadium. The dependence on the energy window is less strong for the late transition metals Fe and Ni, as shown respectively in Tables IV and V. For this reason we have adopted the following procedure for defining the 3d band: it is defined to be those states from the

Energy window (eV)	$U$ (eV)
(-5.0, 0.5)	3.7
(-5.0, 1.0)	3.7
(-5.0, 2.0)	6.3
(-6.0, 0.5)	3.7

TABLE V :  $U$  of Ni as a function of energy window

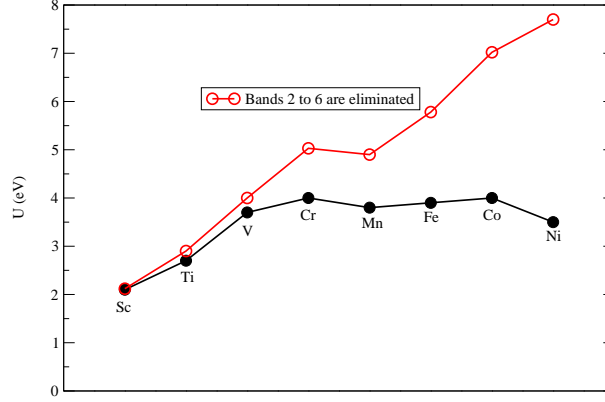


FIG. 8: The Hubbard  $U$  for the 3d series obtained by eliminating transitions among the 3d bands. The empty circles correspond to the case where the 3d bands are defined to be band 2 to 6 and the filled circles to the case where the 3d bands are defined to be band number 2 up to bands below an energy cut off above the Fermi level corresponding to a sharp drop in the 3d density of states, as described in the text. The filled circles are what we define to be the Hubbard  $U$ .

second lowest band (the lowest band is of 4s character), up to states below an energy, just above the Fermi level, corresponding to a sharp drop in the density of states. Figs. 5, 6, and 7 show the partial density of states of V, Fe, and Ni, respectively.

One might wonder if it would not be better to project out the 3d orbitals in calculating  $P_r$  in (3). This procedure turned out to be mathematically unstable resulting in negative static  $U$  and an ad hoc procedure was employed to avoid this problem [19]. It is also tempting to adopt a simple procedure whereby one eliminates bands 2 to 6 (corresponding to the "3d states") when calculating the polarization. This procedure is untenable because band number 6, for example, can be very high in energy, up to 8.0 eV, which clearly cannot be regarded as 3d states. The result using this procedure is illustrated in Fig. 8. The procedure in fact works quite well for the early elements but the result deviates widely from that calculated using the procedure adopted in the present work. The reason for the wide deviation is due to the increasing number of 3d electrons as we go to the later elements. Transitions from the occupied states to unoccupied states just above the Fermi level where the hybridization between the 3d and 4p is strong become increasingly numerous since the number of occupied states increases.

In Fig. 9 the Hubbard  $U$  for the 3d series calculated using the cRPA and cLDA method

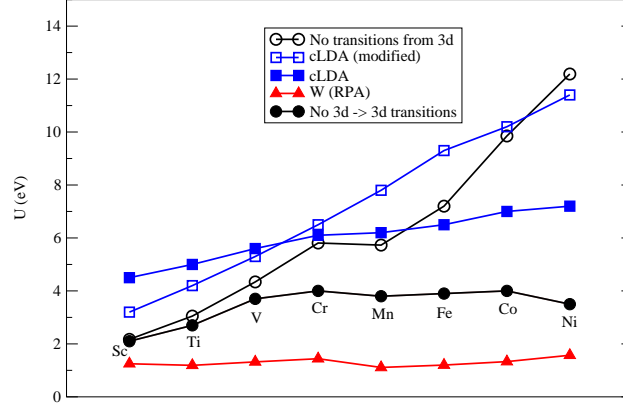


FIG. 9: The Hubbard  $U$  for the 3d transition metal series calculated using the cRPA (filled circle, the same as the filled circles in Fig. 8) and cLDA (filled square). Empty circles correspond to the cRPA result excluding all transitions from the 3d. This should be compared with the modified cLDA result (empty square), as described in the text. For comparison, the fully screened interaction  $W$  is also plotted.

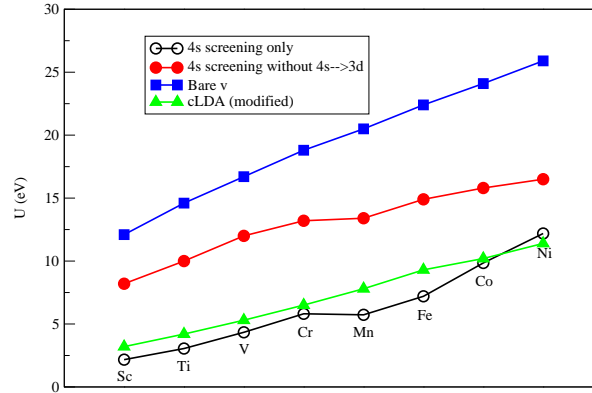


FIG. 10: The effect of orbital contraction across the 3d series. Since the 3d orbital in nickel is most localized the bare Coulomb integral (filled square) is the largest. The bare Coulomb interaction is substantially reduced by the 4s screening (empty circle, the same as the empty circles in Fig. 9). The effect of 4s to 3d screening is illustrated by the filled circles. The effect, represented by the difference between the filled circles and the empty circles, is slightly more important in the early than in the late elements, due to the decreasing number of empty 3d states as we go from early to late elements.



is shown. It is instructive to first consider the case when all transitions from the 3d band are eliminated from the polarization (empty circle), i.e., all screening comes from the 4s electrons. Note that we distinguish between transitions from and to the 3d band. The screened interaction increases almost monotonically from the early to late elements. Two factors are responsible for this monotonic increase. Firstly, the 3d orbital contracts as we go from early to late elements. The effect of the contraction is illustrated by the bare Coulomb matrix element in Fig. 10. Since the bare Coulomb interaction is the same for all elements the increase must be due to the orbital contraction. Secondly, as more 3d states are filled as we go from early to late elements the transitions from the 4s to unoccupied 3d states is reduced resulting in larger screened interaction. To see the contribution of 4s to 3d transitions, the  $U$  values without these transitions are plotted in Fig. 10 (filled circle). The curve is somewhat more flat compared with the case where 4s to 3d transitions are included (empty circle) showing larger 4s-3d screening in early elements. The dominant effect, however, originates from orbital contraction. A similar conclusion was reached by Nakamura et al [9].

The values of the Hubbard  $U$  (filled circle) calculated within the cRPA by eliminating 3d to 3d transitions lie between 2-4 eV across the series. It increases from the early transition metal Sc and reaches a maximum in the middle of the series (Cr, Mn). Compared to the case with 4s screening only (empty circle) we have additional screening channels arising from transitions from 3d to non-3d bands. Evidently in Sc, due to the small number of 3d electrons, these additional screening channels contribute little to screening. As the number of 3d electrons increases, these additional channels correspondingly increase their contribution to screening reaching a maximum in nickel. In the case of nickel, this contribution is so large that when eliminated the bare Coulomb interaction is only reduced to about 12 eV from the bare value of 25 eV. This is in stark contrast to Sc where the screened interaction without contribution to screening from the 3d electrons is close to the value of the fully screened interaction  $W$ , implying that the small number of 3d electrons contribute little to screening, as expected. Contrary to intuition, the screening for  $U$  in transition metals is not only affected by the 4s electrons but also by the 3d electrons, especially in the late transition elements.

We now include the remaining 3d to 3d transitions to reach the fully screened interaction  $W$  (triangle). Not surprisingly, the largest contributions from 3d to 3d transitions occurs

around the middle of the series where the 3d band is half-filled while the early elements show smaller contribution. The late elements also show tendency for smaller 3d to 3d contribution although not as small as for the early elements. It is remarkable although not surprising that the fully screened interaction  $W$  is almost constant across the series. The fact that  $W$  is almost constant across the series can be understood generally in terms of metallic screening. Since metallic screening is very efficient, essentially independent of the number of 3d electrons, the bare Coulomb interaction is always completely screened. Unlike the case of the bare interaction, the effect of orbital contraction is small because the static screened interaction  $W$  is presumably short range.

The Hubbard  $U$  calculated using the cLDA method is significantly higher ( $> 2$  eV) than the value obtained using the RPA. This is rather puzzling because intuitively the procedure employed in the cLDA method is physically equivalent to that of the cRPA (apart from the neglect of exchange-correlation, which is not expected to play a big role in this case and which can be incorporated within the LDA if necessary [20]). One possible source of difference may be due to the fact that by constraining the number of 3d electrons on one site in a supercell, one effectively cuts off the hopping from the 3d orbital to other orbitals. In the language of cRPA, this approximately corresponds to prohibiting transitions from the 3d bands to bands other than 3d as well as transitions from non-3d bands to the 3d bands. For the early transition elements, the contribution of these transitions to screening is relatively small because of the small number of 3d electrons. For this reason cLDA result is close to that of cRPA. However, as we approach the late elements, 3d to non-3d transitions contribute very significantly to screening. Since these are neglected in cLDA, the discrepancy between cLDA and cRPA results becomes much larger. This conclusion is however only semi-quantitative. We emphasize that due to the strong hybridization between the 3d and 4s-4p orbitals, it is difficult to make a clear comparison between cLDA and cRPA.

In Figs. 11 and 12 we show the frequency dependence of the Hubbard  $U$  of nickel and vanadium. We have also analyzed the role of the screening channels in these two systems. As already discussed before, the difference between nickel and vanadium when all transitions from the 3d are eliminated is very striking. More surprisingly, eliminating all transitions from the 4s band (triangles) has little effect on the fully screened interaction  $W$  for both Ni and V, implying that 4s screening is not important. On the other hand, when only the 4s electrons are allowed to screen (by eliminating all transitions from the 3d bands (squares)),

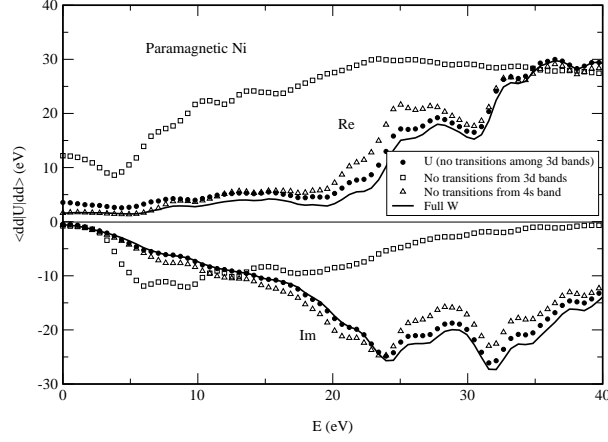


FIG . 11: Frequency dependent  $U$  (filled circle) and  $W$  (solid line) of paramagnetic nickel. Also shown are the results when all transitions from the 3d bands are eliminated (square) and when all transitions from the 4s band (lowest band) are eliminated (triangle).

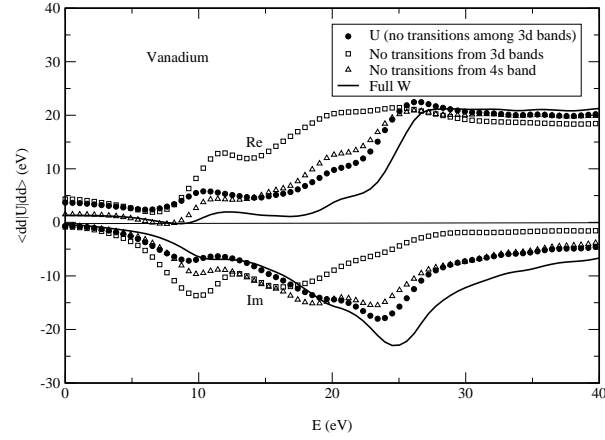


FIG . 12: The same as Fig. (11) but for vanadium .

the bare interaction is reduced from about 25 eV to 12 eV in the case of nickel, and from 20 eV to 4 eV in the case of vanadium , implying the importance of 4s screening. The results appear at first sight to be contradictory but these results reflect the fact that the screening process is "non-additive" in the sense that the effect of screening depends on what is to be screened. When the bare Coulomb interaction is already screened by the 3d electrons, the 4s electrons have little left to screen and vice versa when the 4s electrons have performed the screening there is not much left for the 3d electrons to screen .

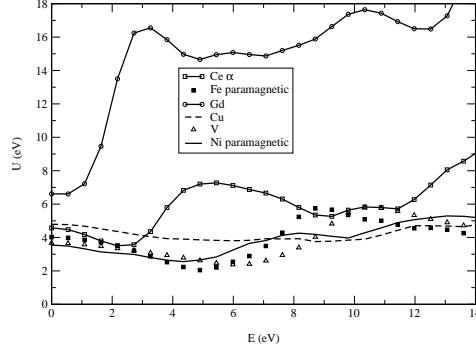


FIG. 13: Frequency-dependent  $U$  of Ce, Fe, Gd, Cu, V, and Ni.

#### D. Breathing or relaxation effects

Finally we comment on relaxation effects of the orbitals on the cLDA method. In calculating  $U$  the corresponding (localized) orbitals are usually allowed to breathe or relax in a self-consistency cycle. Constraining the number of electrons occupying the given orbitals is physically equivalent to applying a perturbing potential acting only on those orbitals such that the occupation number remains constant. The relaxation of the orbitals can therefore be regarded as the response to this perturbing potential. Since hopping from, say, the 3d orbitals is cut off, there are no relaxation to other non-3d orbitals and the relaxation corresponds therefore to (in the RPA language) transitions between 3d-3d, 3d-4d, etc. Transitions from 3d to higher d should be included but at least for the case of nickel, 3d-4d transitions contribute little to the screening of  $U$ . This is in contrast to the atomic case where 3d-4d transitions can be significant [21]. However, 3d-3d transitions should not be allowed since they are implicit in the Hubbard model. The effect of 3d-3d screening can be large since this screening is metallic and may fortuitously compensate for the missing transitions to and from non-3d band. For this reason, we think that cLDA calculations for solids should not include relaxation of the constrained orbitals, as done in the modified cLDA in the present work.

#### E. Frequency dependence of $U$

Finally we comment on the possible importance of energy dependence of  $U$ . In Fig. 13 we show the frequency dependence of  $U$  for some elements within a relatively low energy

range. It becomes clear from the figure that  $U$  can be far from a constant within the bandwidth of each element. This suggests that taking the static value of  $U$  and using it in a model Hamiltonian may be inappropriate. Rather, some kind of averaging over some range of frequency may be necessary. Consider for example cerium. The commonly used value of 6 eV for  $U$  in model calculations falls within the minimum and the maximum value within a frequency range of 5 eV. For iron, the calculated static value of about 4 eV is considerably larger than the commonly used value of 2.0-2.5 eV, which lies in between the calculated static value and the minimum of 2.0 eV at about  $\omega = 5$  eV. The case of Gd is even more striking, with  $U$  starting at 6.5 eV and shooting up to 16 eV within a frequency range of 3 eV. On the other hand, nickel and  $\text{SrVO}_3$  appear to have a relatively constant value of  $U$  at low energy.

#### IV. SUMMARY AND CONCLUSION

We have calculated the Hubbard  $U$  for the 3d transition metal series as well as cerium,  $\text{SrVO}_3$  and  $\text{YTiO}_3$  using a recently proposed basis-independent cRPA method. Although the  $U$  values presented in this work may not be the ultimate ones, we nevertheless believe that they provide a useful guideline for reasonable values of  $U$  that should be used in the lattice Hubbard model. The precise values of  $U$  depends on the choice of the one-particle orbital defining the annihilation and creation operators of the model Hamiltonian, no matter what method we use to calculate  $U$ . Our scheme, however, allows the calculation of  $U(r; r^0)$ , which is basis-independent. But the matrix element in Eq. (5) entering the Hubbard model will inevitably depend on the choice of the one-particle basis  $\phi_{3d}$  of the model.

We have studied systematically the role of the screening channels in a number of materials. In the case of cerium,  $5d \rightarrow 4f$  polarization is important whereas  $4f \rightarrow \text{non-}4f$  is much less important due to a small number of 4f electrons. In the case of  $\text{SrVO}_3$ ,  $O_{2p} \rightarrow V_{3d(t_{2g})}$  polarization plays a crucial role in reducing the Coulomb interaction. On the other hand,  $t_{2g} \rightarrow e_g$  polarization is not important. The screening properties of the 3d transition series are more difficult to analyze due to strong hybridization between the 3d and 4s-4p orbitals, which prevents a clear distinction between the various screening channels. Nevertheless, our results indicate that in early transition series, such as vanadium, most of the (static) screening of  $U$  can be attributed to the 4s electrons. The situation is very different for the

late transition metals, where, in addition to the 4s electrons, the 3d electrons themselves contribute substantially to the screening of  $U$ . This can be understood from a simple fact that the number of 3d electrons is large so that 3d  $\rightarrow$  non-3d screening is substantial, in contrast to the early transition metals with a small number of 3d electrons. For the fully screened interaction  $W$ , 3d  $\rightarrow$  3d screening alone is sufficient to obtain the static value due to a very efficient metallic screening for all the elements in the series. Screening from the 4s electrons alone are not sufficient to obtain the static  $W$ , contrary to what is commonly stated in the literature.

We have also studied the frequency dependence of  $U$  and found that it can be far from constant at low energy. This suggests that for some materials the calculated static value of  $U$  may not be appropriate and some kind of averaging over a frequency range may be necessary. For example, a simple energy averaging over the band width is a possible choice.

We have also compared the cRPA values with those calculated using the well-known cLDA method. Significant discrepancy is observed particularly towards the end of the 3d series. A possible source of discrepancy may be attributed to technical difficulties of including polarization of the 3d electrons to other angular momenta in the cLDA method. We would like to emphasize that the two methods, cLDA and cRPA, theoretically ought to give the same results. In practical implementations, 3d  $\rightarrow$  non-3d polarization corresponding to transitions from the occupied 3d bands to unoccupied bands other than of 3d characters may not be properly included due to the constraint on the number of the 3d electrons, which effectively cuts off hopping of the 3d electrons to other bands. While this polarization is small for the early 3d elements, due to the small number of 3d electrons, the contribution becomes increasingly large as we go towards the end of the series. Our cRPA results for Ce and  $\text{SrVO}_3$  are also consistent with the cLDA results but only when the screening channels associated with the cut off of the hopping in cLDA are correspondingly eliminated. It would be desirable to modify the cLDA method to include screening channels not included in current implementations.

## V. ACKNOWLEDGMENT

Stimulating and fruitful discussions with O. Gunnarsson and K. Nakamura are gratefully acknowledged. F.A. acknowledges the support from NAREGIN anoscience Project, Ministry

- [1] L. Hedin, Phys. Rev. 139, A 796 (1965); L. Hedin and S. Lundqvist, Solid State Physics vol. 23, eds. H. Ehrenreich, F. Seitz, and D. Tumbull (Academic, New York, 1969)
- [2] F. Aryasetiawan and O. Gunnarsson, Rep. Prog. Phys. 61, 237 (1998).
- [3] D. Pines, Elementary Excitations in Solids (Benjamin, New York), (1963).
- [4] O. Gunnarsson, O. K. Andersen, O. Jepsen, and J. Zaanen, Phys. Rev. B 39, 1708 (1989); O. Gunnarsson, Phys. Rev. B 41, 514 (1990); V. I. Anisimov and O. Gunnarsson, Phys. Rev. B 43, 7570 (1991)
- [5] A. K. McMahan, R. M. Martin and S. Satpathy, Phys. Rev. B 38, 6650 (1988)
- [6] M. S. Hybertsen, M. Schluter and N. E. Christensen, Phys. Rev. B 39, 9028 (1989)
- [7] I. V. Solov'yev and M. Imada, Phys. Rev. B 71, 045103 (2005)
- [8] M. Cococcioni and S. de Gironcoli, Phys. Rev. B 71, 035105 (2005)
- [9] K. Nakamura, R. Arita, Y. Yoshimoto, and S. Tsuneyuki, cond-mat/0510425
- [10] M. Springer and F. Aryasetiawan, Phys. Rev. B 57, 4364 (1998)
- [11] F. Aryasetiawan, M. Imada, A. Georges, G. Kotliar, S. Biermann and A. I. Lichtenstein, Phys. Rev. B 70, 195104 (2004)
- [12] O. K. Andersen, Phys. Rev. B 12, 3060 (1975); O. K. Andersen, T. Saha-Dasgupta, S. Erzhov, Bull. Mater. Sci. 26, 19 (2003))
- [13] O. K. Andersen and T. Saha-Dasgupta, Phys. Rev. B 62, R16219 (2000)
- [14] N. Marzari and D. Vanderbilt, Phys. Rev. B 56, 12847 (1997)
- [15] J. F. Janak, Phys. Rev. B 18, 7165 (1978)
- [16] P. Hohenberg and W. Kohn, Phys. Rev. 136, B 864 (1964); W. Kohn and L. Sham, Phys. Rev. 140, A 1133 (1965).
- [17] U. von Barth in The Electronic Structure of Complex Systems, Advanced Study Institute, Vol. 113 of NATO series B: Physics, eds. P. Phariseau and W. M. Temmerman (Plenum, New York, 1982) p.67.
- [18] E. Pavarini, S. Biermann, A. Poteryaev, A. I. Lichtenstein, A. Georges, and O. K. Andersen, Phys. Rev. Lett. 92, 176403 (2004)
- [19] T. Kotani, J. Phys: Condens. Matter 12, 2413 (2000)

- [20] We have done modified cLDA calculations according to Eq. (11), using a  $V(r)$  without the exchange-correlation contribution, and the change is indeed minor (less than 0.2 eV).
- [21] O. Gunnarsson and O. Jepsen, Phys. Rev. B 38, R 3568 (1988)